

Patterning of Si(001) with halogens: Surface structure as a function of the halogen chemical potential

G. A. de Wijs¹ and A. Selloni²

¹*Electronic Structure of Materials, Research Institute for Materials, Faculty of Sciences, Toernooiveld 1, NL-6525 ED Nijmegen, The Netherlands*

²*Department of Chemistry, Princeton University, Princeton, New Jersey 08544*

(Received 22 March 2001; published 29 June 2001)

Chlorine- and bromine-chemisorbed Si(001) surfaces at various coverages (θ) are studied using first-principles density functional calculations. Different stable reconstructions are obtained for the two halogen species. At $\theta=0.5$, Br stabilizes a $c(4\times 2)$ reconstruction with adatoms only on next-nearest neighbor dimers, whereas Cl stabilizes a $p(4\times 2)$ structure with alternating fully chlorinated and empty dimer rows. At $\theta=1$, a 3×2 reconstruction consisting of dimer rows separated by missing atom rows is most stable for Br, whereas for Cl such a structure is degenerate with the conventional 2×1 reconstruction. These findings are in agreement with recent scanning tunneling microscopy experiments. They can be rationalized on the basis of a stronger steric hindrance for Br.

DOI: 10.1103/PhysRevB.64.041402

PACS number(s): 68.43.-h

The interactions of Si(001) with halogens have been widely studied mostly because of the importance of halogen etching in VLSI technology. In a series of papers, Weaver and co-workers have studied the surface morphology of chlorine- and bromine-etched Si(001) with scanning tunneling microscopy (STM).¹⁻³ They found an interesting difference between Cl and Br at high coverage: while on Si(001)-Cl the usual 2×1 dimer structure is generally observed, Br stabilizes a surface reconstruction with apparent 3×1 periodicity.^{1,3} STM images of the “ 3×1 ” reconstructed regions show bright rows of Br-saturated silicon dimers separated by dark rows that are a single atom wide. The potential use of this patterned structure as a template for overlayer growth is of considerable interest.

To explain the “ 3×1 ” reconstruction, Chander *et al.*¹ suggested that on the Br-covered surface a structure similar to that of hydrogen on Si(001) could form at high coverage. For Si(001)-H a 3×1 reconstruction is known to occur,⁴⁻⁶ which consists of rows of fully hydrogenated Si dimers alternating with rows of SiH₂ species, corresponding to a H-coverage of 4/3. However, contrary to SiH₂, the SiBr₂ units are volatile at the relatively high temperatures (~ 800 K) at which the transition to the 3×1 is observed. It was thus proposed that these species desorb, leaving a 3×1 structure of dimer rows separated by trenches of missing atom rows.

However, the possibility that a Si(001)-Br(3×1) structure with 4/3 coverage forms, even temporarily, is not obvious, e.g., important repulsive interactions are present between the adsorbed Br atoms on the Si(001) surface. Evidence of such repulsive interactions is provided by a recent STM study of Herrmann and Boland.⁷ Under appropriate preparation conditions, and at about half coverage, Br adatoms are found to form a $c(4\times 2)$ phase in which they occupy alternating dimers along a row with an out-of-phase occupancy between adjacent rows, so as to maximize the distances between adatoms in different dimers.

In order to provide a theoretical basis for these experimental observations, in this Rapid Communication we inves-

tigate the surface structure and stability of Si(001)-X ($X = \text{Cl, Br}$) at various X -coverages (θ_X) via first-principles density functional calculations. Following the procedure used by Northrup⁶ for the hydrogenated Si(001) surface, we calculate surface formation energies as a function of the halogen chemical potential (μ_X). The questions we primarily address concern the “degree of stability” of the $c(4\times 2)$ and “ 3×1 ” surface phases imaged by STM on Si(001)-Br, i.e., are there well defined ranges of μ_{Br} in which these structures are indeed the most stable? Are there competing phases which are energetically close? What are the similarities and differences between the chlorine- and bromine-covered surfaces? What are the detailed atomic geometries of the $c(4\times 2)$ and “ 3×1 ” phases?

Our results agree well with the available experimental information, confirming in particular the different behavior of the Cl- and Br-covered Si(001) surfaces. For Si(001)-Br, we find a small region of chemical potential (corresponding to intermediate coverage) where the most stable phase is a $c(4\times 2)$ structure qualitatively identical to that described by Herrmann and Boland,⁷ while at higher μ_{Br} (coverage) a “ 3×1 ” (in fact a 3×2) patterned surface is more stable than the 2×1 , by ~ 15 meV/(1×1). For Si(001)-Cl, a $p(4\times 2)$ phase, consisting of alternating fully chlorinated and completely empty dimer rows, is found to be the most stable at half coverage, while at monolayer coverage, the “ 3×1 ” and 2×1 reconstructions are energetically degenerate. This difference in behavior between Cl and Br indicates that both the electrostatic repulsive interactions between adsorbed atoms, and their “size,” are important in determining the patterning of the halogenated Si(001) surface.

Calculations have been performed with the first-principles molecular-dynamics program VASP (Vienna *ab initio* simulation program)⁸ using density functional theory in both the local density (LDA)⁹ and the generalized gradient approximation (GGA) by Perdew *et al.*¹⁰ Below we report GGA results only.¹¹ Electron-ion interactions were described using ultra-soft pseudopotentials^{12,13} for Cl and Br, and a norm-

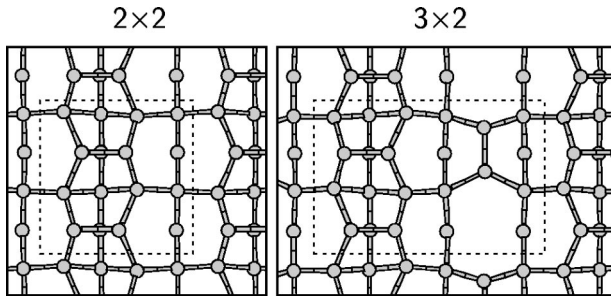


FIG. 1. Top view along $[0,0,\bar{1}]$ of the Si(001) surfaces with $p(2\times 2)$ (left) and 3×2 (right) surface unit cells. Dashed lines indicate the boundaries of the irreducible surface unit cells. Only atoms in the four upper atomic layers are shown.

conserving pseudopotential for Si.¹⁴ The nonlocal projections of the pseudopotentials were carried out in real-space,¹⁵ and nonlinear core corrections were applied to all elements.¹⁶ The kinetic energy cutoff on the wave functions was 375 eV (27 Ry). The surfaces were modeled using a (periodically repeated) slab with 12 atomic layers of Si. Cl or Br are adsorbed on both sides of the slab. Identical surfaces on both sides of the slab were enforced by a twofold rotation axis at the center of the slab. All atoms were allowed to relax. The cell dimensions along z and y were fixed by the calculated bulk lattice constant ($a_0 = 5.460$ Å), whereas the slabs were separated from their periodic images by a vacuum region of approximately 10 Å. Consistent sets of k points were used for the different surface cells and the convergence of the k -space sampling was carefully checked.¹⁷

The surface formation energies E_{form} , at zero temperature and neglecting quantum effects, were calculated as

$$E_{\text{form}} = E_{\text{slab}} - n_{\text{Si}} \mu_{\text{Si}} - n_X \mu_X,$$

where E_{slab} is the total energy of the supercell, and n_{Si} and n_X are the number of silicon atoms and halogen adatoms, respectively. μ_{Si} and μ_X are their respective chemical potentials. As Si is in equilibrium with its bulk, μ_{Si} equates the bulk total energy per atom. The halogen chemical potential, which is allowed to vary, will be measured relative to the value for which the formation energy of the $\text{Si}X_4$ molecule is zero.

First we consider the clean surface, i.e., $n_X = 0$. We use a 2×2 surface unit cell, so that the lowest energy structure is the $p(2\times 2)$ pattern (see Fig. 1) in which neighboring surface dimers along a row buckle in opposite directions. We also examine a “ 3×1 ” reconstruction, consisting of alternating dimer rows and missing atom rows, analogous to the model proposed by Weaver and co-workers for the brominated surface.^{1,3} To model this structure, a 3×2 cell is used to accommodate the alternate buckling of the dimer row. Upon relaxation a dimerization of the exposed second layer atoms (in the missing atom row) takes place, so that a truly 3×2 , rather than 3×1 , reconstruction is present (see Fig. 1). As expected, this 3×2 reconstruction has a higher formation energy, 1.200 eV/(1×1 cell), than the 2×2 , 1.184 eV/(1×1 cell) (see Fig. 4). From this result we can estimate the formation energy E_A of an S_A step, as the miss-

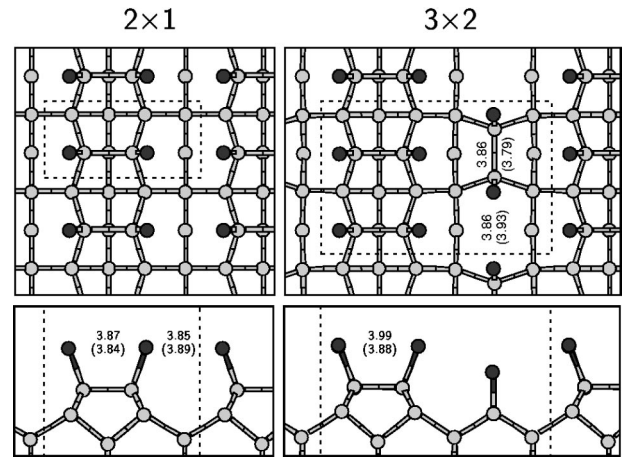


FIG. 2. Top and side views of Br-covered Si(001) surfaces at $\theta_{\text{Br}} = 1$ with the 2×1 (left) and 3×2 (right) surface unit cells, seen along $[0,0,\bar{1}]$ and $[\bar{1},1,0]$ respectively. In all plots $[1,1,0]$ runs from left to right. The dark spheres represent Br atoms, the others Si atoms. Only the four Si layers nearest to the surface are shown. Br-Br distances are indicated, with the analogous Cl-Cl distances in brackets.

ing row feature in the 3×2 can, in essence, be considered as two S_A steps. We obtain $E_A = 0.048$ eV/ $2a$, where $2a = \sqrt{2}a_0$ is the length of the 2×2 surface unit cell. This compares very well to experimental values for single S_A steps that are in the range 0.052 to 0.064 eV/ $2a$.¹⁸ Although this good agreement could be to some extent fortuitous because the steps in the 3×2 structure are very close to one another,¹⁹ it suggests however that the difference between the 3×2 and 2×2 formation energies is reasonably well given by our calculations.

For the Cl- and Br-covered surfaces, several structural models with different coverages $\mu_X \geq 0.5$ have been examined. At monolayer coverage (see Fig. 2), we considered the usual 2×1 reconstruction with all dimers saturated by halogens, and the 3×2 patterned surface obtained by saturating the 3×2 model of Fig. 1. For Si(001)-Br, the latter is favored by ~ 15 meV/(1×1), whereas for Si(001)-Cl the two structures are substantially degenerate. The difference between the Cl- and Br-terminated surfaces can be rationalized in terms of a combination of electrostatic and steric repulsion effects.²⁰ In the 2×1 reconstruction, the Br-Br (Cl-Cl) intradimer distance is 3.87 (3.84) Å whereas in the 3×2 surface this is 3.99 (3.88) Å for the atoms on the dimer rows and 3.86 (3.79) Å for the atoms in the trench. Thus the Cl-Cl distances are similar on both surfaces, but on the 3×2 two thirds of the Br-Br distances increase by more than 0.1 Å. In fact, on the 2×1 surface the Br-Br distance cannot be further relaxed because the Br atoms on the adjacent dimer rows are too close (3.85 Å). Thus a surface stress is built up. In the 3×2 surface the distance to the Br atoms in the trench is much larger (~ 4.4 Å), so that the Br atoms on the dimer rows are able to relax outwards and release part of the stress.

At half coverage (see Fig. 3), a $p(4\times 2)$ structure is the most stable for Cl, while for Br the $c(4\times 2)$, as seen by

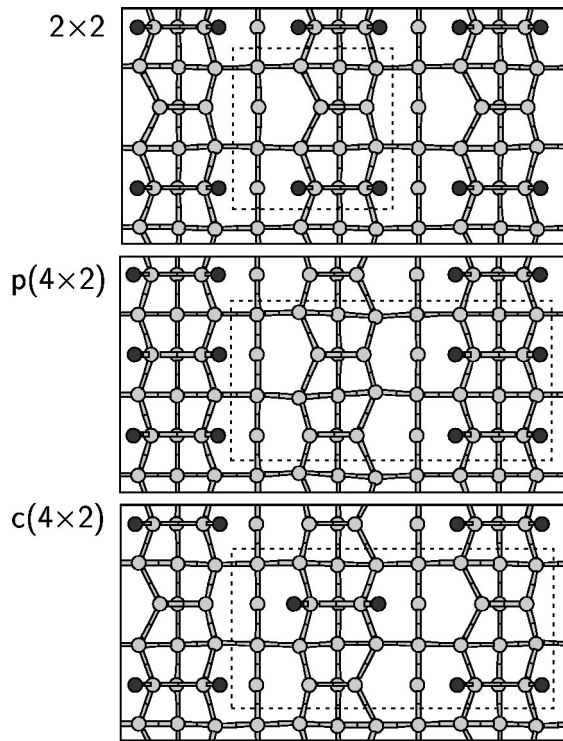


FIG. 3. Top views of Br-covered surfaces at $\theta_{\text{Br}}=0.5$. The dark spheres represent Br atoms, the others Si atoms. Only the four Si layers nearest to the surface are shown. The intradimer Br-Br distances are 3.87, 4.07, and 4.08 Å for the 2×2 , $c(4\times 2)$, and $p(4\times 2)$ reconstructions, respectively. For the analogous Cl covered surfaces these distances are 3.82, 3.89, and 3.90 Å.

STM,⁷ is favored. This indicates the presence of steric repulsions between Br adatoms on neighboring dimers along a row. As the shortest interdimer Br-Br distance in the $c(4\times 2)$ surface is 5.3 Å, electrostatic interdimer repulsions are small, so that the intradimer Br-Br distance can relax to as much as 4.08 Å. A similar $c(4\times 2)$ structure has been observed with iodine, which is even larger than Br.²¹ For the “smaller” Cl adatom, instead, steric effects are less important, so that the $p(4\times 2)$ structure, which does not disrupt the ordered buckling pattern along a row, is preferred to the $c(4\times 2)$.

Finally, we consider the surface formation energies as a function of μ_X (see Fig. 4). For $\theta=0$, we report E_{form} of the 3×2 and 2×2 structures of Fig. 1, as well as that of the clean $c(4\times 2)$ buckled surface, that we estimate from the results of Ref. 22. From Fig. 4, we can see that for both halogens, but especially for Br, there is a small interval of μ_X where one of the half coverage structures is the most stable (see inset). For Si(001)-Br this is the $c(4\times 2)$ structure in Fig. 3. For the brominated surface, besides the half and full monolayer structures described above, we also consider a 3×2 surface with $\theta_{\text{Br}}=2/3$ (obtained by removing the halogen adatoms on the second layer dimers of Fig. 2), and a 3×1 structure with $\theta_{\text{Br}}=4/3$ (formed by rows of halogenated dimers separated by rows of SiBr_2 units). The 3×2 surface with $\theta=2/3$ is always thermodynamically unstable, while the 3×1 reconstruction with $\theta=4/3$ becomes

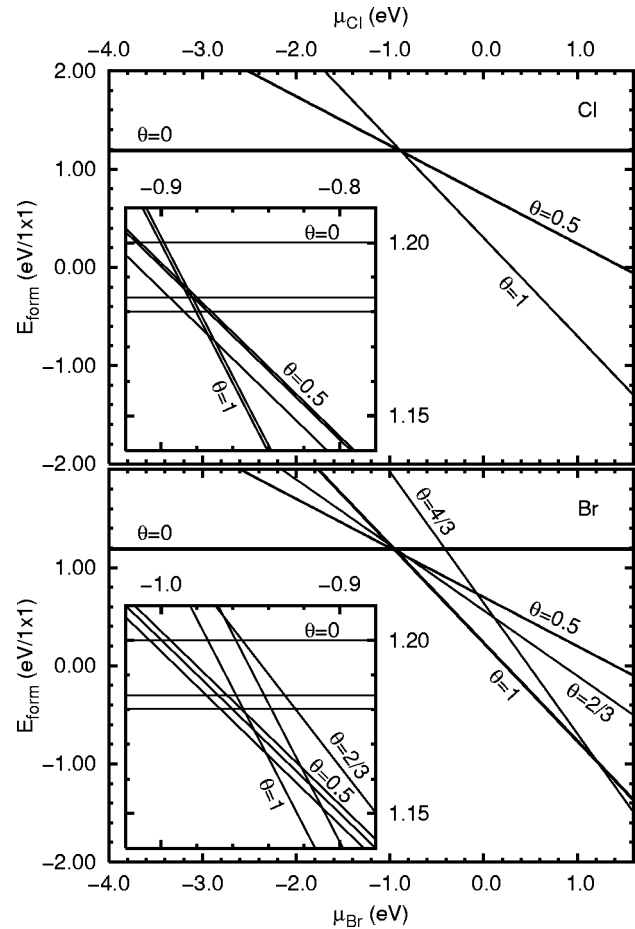


FIG. 4. Formation energies of surface reconstructions as a function of halogen chemical potential for Si(001)-Cl (upper panel) and Si(001)-Br (lower panel). The insets show a blow-up of the region where different lines intersect. The three horizontal lines ($\theta=0$), in order of decreasing formation energy, correspond to the 3×2 , $p(2\times 2)$, and $c(4\times 2)$ reconstructions. The energy difference between the latter two was taken from Ref. 22. For $\theta=0.5$, in order of decreasing formation energy, the lines correspond to the $c(4\times 2)$, 2×2 (nearly degenerate), and $p(4\times 2)$ reconstructions for Cl and to the 2×2 , $p(4\times 2)$, and $c(4\times 2)$ reconstructions for Br. For $\theta=1$, in the same order, the lines correspond to the 2×1 and 3×2 reconstructions for both Cl and Br. The lines at $\theta=2/3$ and $\theta=4/3$ pertain to the 3×2 without Br in the missing atom row and the 3×1 with rows of Br-saturated dimers alternating with rows of SiBr_2 units, respectively.

favorable at high positive values of μ_{Br} , i.e., it may form under extreme conditions only.

Although our calculations indicate that at full monolayer Br coverage, the 3×2 structure is thermodynamically most favorable, its formation from the usual 2×1 reconstruction requires a rearrangement of the upper layer of Si atoms. This may be kinetically inhibited, i.e., a metastable 2×1 may exist. Indeed, in their STM experiments Herrmann and Boland⁷ observe the 2×1 reconstruction at monolayer coverage. Weaver and co-workers only observe the transition to the “ 3×1 ” at relatively high coverage ($\theta\geq 0.8$) and temperatures so high (~ 800 K) that even etching occurs.^{1,3}

For Si(001)-Cl, the range of μ_{Cl} in which the half cover-

age $p(4\times 2)$ surface appears to be stable is even smaller than for Si(001)-Br, while at higher μ_{Cl} the 2×1 and 3×2 reconstructions with monolayer coverage are equally stable. Thus the thermodynamic driving force for a $2\times 1\rightarrow 3\times 2$ transition is much smaller than for Br. This is consistent with that fact that the 3×2 is almost never seen on Si(001)-Cl, although a full explanation would also need to consider the kinetics of this transition.

In conclusion, our calculations show that for Si(001)-Br $c(4\times 2)$ and 3×2 structures are thermodynamically favored around half and full monolayer coverage, respectively. Although the 3×2 structure of this work is slightly different with respect to the model originally proposed by Chander *et al.*,¹ we found that it yields an STM image very similar to the one observed experimentally.²³ We thus propose that the

experimental image actually corresponds to the 3×2 structure that we calculate. The $c(4\times 2)$ phase is stable in a narrow range of Br chemical potential, which seems consistent with the fact that special care is needed to observe it experimentally.⁷ Finally our results provide a rationalization of the different behavior of Si(001)-Cl and Si(001)-Br in terms of a combination of electrostatic and steric repulsion effects. The transition at high coverage from the 2×1 to the 3×2 reconstruction is kinetically limited. This mechanism poses interesting questions for future work.³

This work is part of the research program of the Stichting voor Fundamenteel Onderzoek der Materie (FOM) with financial support from the Nederlandse Organisatie voor Wetenschappelijk Onderzoek (NWO).

-
- ¹M. Chander, Y. Z. Li, D. Rioux, and J. H. Weaver, Phys. Rev. Lett. **71**, 4154 (1993).
- ²M. Chander, Y. Z. Li, J. C. Patrin, and J. H. Weaver, Phys. Rev. B **47**, 13 035 (1993); D. Rioux, M. Chander, Y. Z. Li, and J. H. Weaver, *ibid.* **49**, 11 071 (1994); D. Rioux, R. J. Pechman, M. Chander, and J. H. Weaver, *ibid.* **50**, 4430 (1994); K. Nakayama, C. M. Aldao, and J. H. Weaver, Phys. Rev. Lett. **82**, 568 (1999).
- ³K. Nakayama, C. M. Aldao, and J. H. Weaver, Phys. Rev. B **59**, 15 893 (1999).
- ⁴Y. J. Chabal and K. Raghavachari, Phys. Rev. Lett. **54**, 1055 (1985).
- ⁵J. J. Boland, Phys. Rev. Lett. **65**, 3325 (1990).
- ⁶J. E. Northrup, Phys. Rev. B **44**, 1419 (1991).
- ⁷C. F. Herrmann and J. J. Boland, Surf. Sci. **460**, 223 (2000).
- ⁸G. Kresse and J. Hafner, Phys. Rev. B **47**, 558 (1993); **49**, 14 251 (1994); G. Kresse and J. Furthmüller, Comput. Mater. Sci. **6**, 15 (1996); G. Kresse and J. Furthmüller, Phys. Rev. B **54**, 11 169 (1996).
- ⁹D. M. Ceperley and B. J. Alder, Phys. Rev. Lett. **45**, 566 (1980).
- ¹⁰J. P. Perdew, J. A. Chevary, S. H. Vosko, K. A. Jackson, M. R. Pederson, D. J. Singh, and C. Fiolhais, Phys. Rev. B **46**, 6671 (1992).
- ¹¹Calculations with the LDA were carried out for the clean and several halogenated surfaces. They confirm the GGA results.
- ¹²D. Vanderbilt, Phys. Rev. B **41**, 7892 (1990).
- ¹³G. Kresse and J. Hafner, J. Phys.: Condens. Matter **6**, 8245 (1994).
- ¹⁴A. M. Rappe, K. M. Rabe, E. Kaxiras, and J. D. Joannopoulos, Phys. Rev. B **41**, 1227 (1990).
- ¹⁵R. D. King-Smith, M. C. Payne, and J. S. Lin, Phys. Rev. B **44**, 13 063 (1991); G. Kresse (unpublished).
- ¹⁶S. G. Louie, S. Froyen, and M. L. Cohen, Phys. Rev. B **26**, 1738 (1982).
- ¹⁷Optimizations on the 2×1 , 3×1 , 2×2 , and 3×2 cells were carried out with \mathbf{k} -point meshes equivalent to a $6\times 6\times 1$ mesh 24 for a 1×1 surface unit cell. For the 4×2 and 2×2 cells with $\theta_x=0.5$ meshes equivalent to $8\times 8\times 1/1\times 1$ cell were used. Final total energies were obtained from single point calculations with meshes equivalent to $12\times 12\times 1/1\times 1$. Symmetry was exploited and only irreducible \mathbf{k} -points were used.
- ¹⁸H. J. W. Zandvliet, Rev. Mod. Phys. **72**, 593 (2000), and references therein.
- ¹⁹D. R. Bowler and M. G. Bowler, Phys. Rev. B **57**, 15 385 (1998).
- ²⁰As a confirmation of the relevance of steric effects, notice that for Si(001)-H the 2×1 structure is found to be more stable than the 3×2 one by ~ 9 meV/(1×1) cell.
- ²¹D. Rioux, F. Stepniak, R. J. Pechman, and J. H. Weaver, Phys. Rev. B **51**, 10 981 (1995).
- ²²P. Bogusławski, Q.-M. Zhang, Z. Zhang, and J. Bernholc, Phys. Rev. Lett. **72**, 3694 (1994).
- ²³The Br atoms in the trench are too deep into the surface to be imaged.
- ²⁴H. J. Monkhorst and J. D. Pack, Phys. Rev. B **13**, 5188 (1976).